Kinetic study and simulation of molybdenum borides for hydrogen evolution reaction

**Harunal Rejan Ramji[1,2], Muhammad Qhaliff Zainal Ibidin[1], Nicolas Glandut[2],
Joseph Absi[2], Lim Soh Fong[1]**

[1]Department of Chemical Engineering and Energy Sustainability, Faculty of Engineering, Universiti Malaysia Sarawak (UNIMAS),
Kota Samarahan, Malaysia
[2]Institute for Research on Ceramics (IRCER) UMR 7315, CNRS, University of Limoges, European Ceramics Center, Limoges, France

ABSTRACT

This paper presented the kinetic study of molybdenum borides via the Volmer-Heyrovsky-Tafel (V-H-T) mechanistic steps for hydrogen evolution reaction (HER). A theoretical approach was carried out to investigate the kinetic properties of several molybdenum boride materials for HER in 0.5 M H2SO4. Our findings offer definitive proof that the simulated results show that B, Mo, Mo2B, and α-MoB, proceed through V-H mechanistic steps (slower kinetics) while β-MoB and MoB2 exhibit V-H-T mechanistic steps with higher kinetics. The kinetic parameters were determined in terms of the standard rate constant parameters for the Volmer step (kV, k-V), Heyrovsky step (kH, k-H), and rate constant for the Tafel step (kT, k-T). The simulation was able to predict the overpotential at 10 mA/cm2, η10 recorded at approximately 780, 585, 480, 350, 310, and 300 mV for B, Mo, Mo2B, α-MoB, β-MoB, and MoB2 respectively. Based on these findings, the adopted mathematical model shows good coherency to the experimental findings. The simulation work provides a good numerical estimation of the characteristics of the electrocatalyst for HER. This paper successfully elucidated the reaction mechanisms (V-H-T steps) and understood the rate-limiting steps involved in the HER process on Mo-B materials.
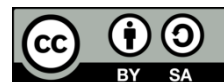
Corresponding Author:

Harunal Rejan Ramji
Department of Chemical Engineering and Energy Sustainability, Faculty of Engineering
Universiti Malaysia Sarawak (UNIMAS)
94300, Kota Samarahan, Sarawak, Malaysia
Email: rhrejan@unimas.my

1. INTRODUCTION

Developing highly efficient HER low-cost electrocatalysts is of utmost importance to realize hydrogen economy. Earth's abundant compounds such as carbons have attracted tremendous research interest. Among them, molybdenum carbides have exhibited great potential catalytic properties [1]–[3]. Recent studies demonstrated the efficacy of boron-containing materials in improving the catalytic activity for hydrogen evolution. It has been discovered that when a boron atom is close to a carbon atom, the valence orbital energy levels of the carbon atom are lowered. Park *et al*. [4] presented The HER activity of B, Mo, Mo_2B, α-MoB, β-MoB, and MoB_2 catalysts. The HER kinetics rise dramatically as the boron concentration rises. The findings demonstrate that boron inclusion had significantly enhanced the molybdenum catalyst.

Jian *et al*. [5] introduce a material of MoO_2 layer on Mo foil, $MoSe_2/MoO_2$ hybrid nanosheets with an abundant edge and high electrical conductivity can be synthesized on the surface of Mo foil to improve HER on the material. The developed MoSe2/MoO2/Mo exhibits highly improved HER performance

compared with that of the pure MoSe₂ catalyst. MoSe2/MoO2/Mo has a small Tafel slope of 48.9 mV dec^{-1}, a low onset potential of 60 mV versus RHE, and a small overpotential of 142 mV versus RHE at a current density of 10 mA/cm^2. The high catalytic activities of MoSe2/MoO2/Mo are ascribed to the synergistic effects of the abundant active sites at the MoSe₂ surface and fast charge transport efficiency between MoSe2 and MoO2/Mo substrate. Similar works on CoS2 were presented by Zhang *et al*. [6] on the positive effect of The study by Zhang *et al*. [7] presented a one-pot approach for manufacturing B-doped RhFe alloy with high catalytic performance for HER. It has been found that the BRF21 catalyst, in its current form, is highly stable in acidic environments. It has remarkable stability and high HER activity in an aqueous solution (0.5 M H₂SO₄), with an initial overpotential that is almost negligible. It requires an overpotential of around 25 mV at a current density of 10 mA/cm^2, which is four mV lower than that of commercial Pt/C (29 mV). In addition, the Tafel slope of 32 mV/dec^1 with Pt/C is similar for BRF21 (30 mV dec^{-1}). Before and after being put through the durability test, the amount of B in its atomic percentage increases from 9.57 to 12.51. These results suggest that boron dopants may be stable in 0.5 M H₂SO₄ aqueous solution. Therefore, boron-doping may be an effective method for boosting HER activity. While electrocatalyst testing in acidic conditions shows tremendous HER activity, the study of electrocatalysts for HER in alkaline condition had also significan progress [8].

Work such as Danaee and Noori [9] stated that the HER of 1T MoS₂ nanosheets happens mainly via the Volmer-Heyrovsky mechanism. Azizi *et al*. [10] presented that the HER mechanism for tin at low negative potentials is a serial combination of the Volmer step and parallel Tafel and Heyrovsky steps. At high negative potentials where the hydrogen coverage reaches its limiting value, a Tafel line with a slope of 126 mVdec^{-1} is obtained. In this potential region, the mechanism of the HER follows Volmer–Heyrovsky while the Tafel step has negligible contribution. The kinetic studies indicate that the rate of HER is controlled by the Volmer step. Studies of the HER on nickel boride electrodes doped by Rh, Ru, Co, Cr, Zn and Pt carried out by quasi steady-state galvanostatic experiments and by ac impedance spectroscopy show that the overall electrode reaction proceeds via the Volmer-Heyrovsky mechanism.

One of the primary contributions of this paper is the in-depth kinetic study of molybdenum borides regarding their efficacy in catalyzing the HER. This paper took inspiration from the published works of Luo *et al*. [11], Lasia and Rami [12], Los *et al*. [13], Xu *et al*. [14] to determine the Volmer-Heyrovsky-Tafel (V-H-T) mechanistic steps of B, Mo, Mo₂B, α-MoB, β-MoB, and MoB₂ catalysts for HER in acidic condition. The standard rate constant of these steps will be determined by adopting the VHT model for HER [15]–[17]. The obtained values will be compared to the experimental findings by Park *et al*. [4] on multiple molybdenum borides (Mo₂B, α-MoB, β-MoB, and MoB₂) with increasing HER activity.

2. METHODOLOGY
2.1. Volmer Heyrovsky Tafel mechanistic steps
In general, the basic concept of HER is the cathodic side of the electrochemical splitting of water molecules (H₂O) to H₂ (HER) and O₂ (OER). The overall reaction is represented as in (1), a reaction occurring at the cathode.

$$2H^+ + 2e^- \rightarrow H_2 \tag{1}$$

The elementary steps of HER that occur on the surface of the surface are called the V-H-T mechanism, where (2)-(4) represent V-H-T steps respectively. These reactions could occur simultaneously in either VH, VT, or VHT paths depending on the experimental conditions These steps are depicted in Figure 1.

$$H^+ + s + e^- \rightleftarrows Hs \tag{2}$$

$$H^+ + Hs + e^- \rightleftarrows H_2 + s \tag{3}$$

$$2Hs \rightleftarrows H_2 + 2s \tag{4}$$

2.2. Boundary conditions
V and H are electrochemical reactions and hence are potentially dependent. The rate constants for the forward and the backward reactions are expressed as in (5)-(8).

$$K_V = \left(k_V e^{\left(-\frac{\beta_V nF}{RT}\right)\left(E_{(t)} - E_V^o\right)} \right) \tag{5}$$

$$K_{-V} = \left(k_{-V} e^{\left(\frac{\alpha_V nF}{RT}\right)\left(E_{(t)} - E_V^o\right)} \right) \tag{6}$$

$$K_H = \left(k_H e^{\left(-\frac{\beta_H nF}{RT}\right)\left(E_{(t)} - E_H^o\right)} \right) \tag{7}$$

$$K_{-H} = \left(k_{-H} e^{\left(\frac{\alpha_H nF}{RT}\right)\left(E_{(t)} - E_H^o\right)} \right) \tag{8}$$

Where k_V and k_{-V} are standard rate constants for forward and backward Volmer steps respectively. While K_V and K_{-V} are the rate constants for forward and backward Volmer steps respectively. The subscript H would represent the Heyrovsky step. Since the Tafel step is a chemical reaction, not an electrochemical reaction, hence it is independent of the potential.

The transfer coefficients or symmetry coefficients are represented by β and α in which (α+β=1). The subscripts V and H signify the Volmer and Heyrovsky step respectively. As for the potential parameters, $E_{(t)}$ is the electrode potential, and E^0_V and E^0_H are the standard potentials for Volmer and Heyrovsky respectively. Assuming the Langmuir adsorption isotherm, the reaction rates for the corresponding as in (2)-(4) are presented as (9)-(11) respectively.

$$R_V = (K_V c_{H+} c_s) - (K_{-V} c_{Hs}) \tag{9}$$

$$R_H = (K_H c_{H+} c_{Hs}) - \left(K_{-H} c_{H_2} c_s\right) \tag{10}$$

$$R_T = \left(K_T (c_{Hs})^2\right) - \left(K_{-T} c_{H_2} (c_s)^2\right) \tag{11}$$

Several parameters were kept constant throughout the simulations with the following assumptions:
i)   0.5 M of H_2SO_4 of high acidic concentration, hence $c_{H+}=1000$ mol/m^3.
ii) The maximum surface concentration of the material, $\Gamma_{max}=1 \times 10^{-5}$ mol/m^2 (eg given by Diard et al. [18] and Faulkner et al. [19].
iii) The hydrogen concentration near the electrode is 0.001 M, $c_{H2}=1$ mol/m^3.

Pertaining the c_{H2} an elaborate work by Kempainen et al. [20] had presented the concentration profiles of dissolved H_2 at different current densities. The works stated the change of c_{H2} with the change of current density at different distances near the electrode, but a safe assumption of $c_{H2}=1$ mol/m^3 can be made to achieve a current density of -10 mA/cm^2. To support the assumption made on c_{H2}, Lasia [21] cited a work on solubility series in the year 1981 that stated c_{H2} is estimated at 0.0008 M or 0.8 mol/m^3.

The general PDE equation was employed to facilitate Fick's 2nd law of diffusion. The general form PDE is written in the form of (12).

$$e_a \frac{\partial^2 u}{\partial t^2} + d_a \frac{\partial u}{\partial t} = f \tag{12}$$

Where e_a and d_a are the mass coefficients, Γ is the flux vector and f is the source term. Given that u, in this case, is c_{Hs} in mol/m^2, Fick's 2nd law of diffusion is written in eq. 3.28. The mass coefficient, $e_a=0$ as no second-order derivation of time is required. While $d_a=1$ to facilitate the first-order derivation of c_{Hs}. In steady-state conditions, Fick's 2nd law of diffusion (1st term) and the total rate reaction (the 2nd term) is equal to zero.

$$\frac{\partial c_{Hs}}{\partial t} = R_v - R_H - 2R_T = 0 \tag{13}$$

Based on the work such as (Glandut et al., [22], [23]) the equation for current density for a single electrode system is written in (14). The currents are due to the electron transfer during the Volmer and Heyrovsky steps occurring on the surface of the electrode. By integrating the Volmer and Heyrovsky rate reactions on the electrode surface and the multiplication with Faraday's constant and the number of electrons moving the current equation is written as (15). Similar formulizations can also be found in Compton and Banks [24].

$$i = \frac{I_\sigma}{A_\sigma} = (-nF(R_V + R_H)_\sigma) \tag{14}$$

$$I_\sigma = -nF \int_0^{\sigma_D} \int (R_V + R_H)_\sigma \, d\sigma \qquad (15)$$

Dividing the current over the effective surface area, A_{Tot} would then give the current density, i as shown in the (16). Consequently, the Tafel plot can be obtained by plotting (17) against the potential, $E_{(t)}$.

$$i_{Tot} = \frac{I_{Tot}}{A_{Tot}} \qquad (16)$$

$$\log_{10}(i_{Tot}) = \log_{10} \frac{(I_{TiC} + I_{taC})}{A_{Tot}} \qquad (17)$$

Additionally, the analytical equation provided in (18) can be used to verify the Tafel plot for an irreversible VH mechanism [23].

$$J = 2F\Gamma_{max} c_{H+} \frac{(K_V K_H)}{K_V + K_H} \qquad (18)$$

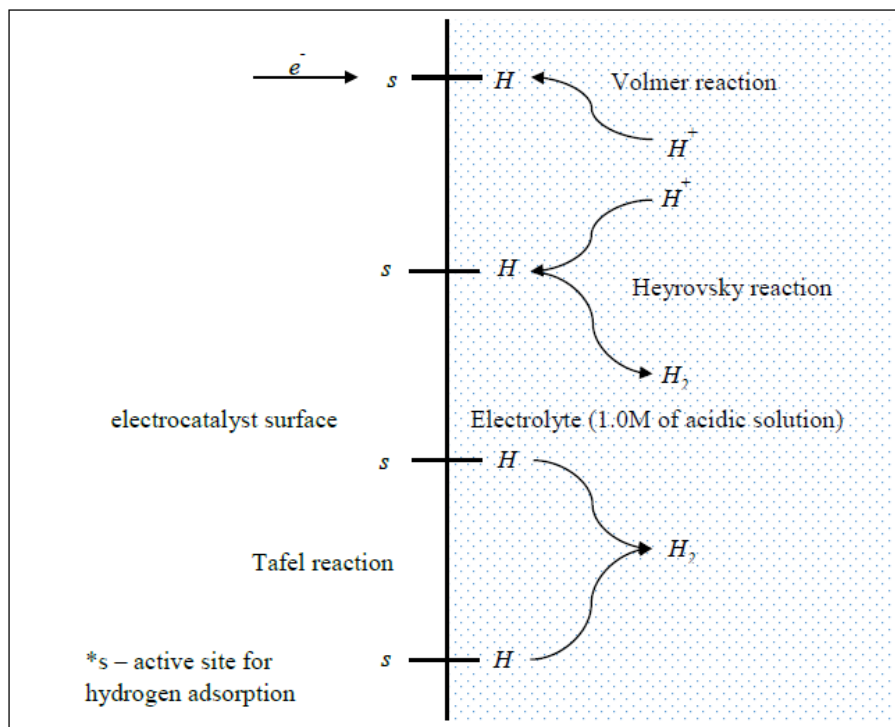The essential parameters in this simulation are summarized in Table 1.

Figure 1. Schematic diagram of a VHT reaction on an electrocatalyst surface

Table 1. Parameters employed for VHT mechanistic steps in the simulation

Name	Expression	Value	Description
n	1	1	No of electron
R	8.314[J/(mol*K)]	8.314 J/(mol·K)	Universal gas constant
T	298.15[K]	298.15 K	Temperature
F	96485.3[C/mol]	96485 C/mol	Faraday's constant
H2	1[mol/m^3]	1 mol/m³	Hydrogen concentration (c_{H2})
vb	1e-8[V/s]	1×10^{-8} V/s	Potential scan rate (v_b)
Einit	0.5	0.5	Initial potential (E_{init})
cstar	1000[mol/m^3]	1000 mol/m³	Initial concentration for H$^+$ (c_{H+})
Gmax	1e-5[mol/m^2]	1×10^{-5} mol/m²	Maximum concentration of Hs (Γ_{max})
tend	2e8	2×10^8	Time stop (t_{end})
tstep	2e5	2×10^5	Time step (t_{step})
Erev	-0.5[V]	-0.5 V	Reverse potential (E_{rev})

2.3. Time-dependent properties

For the time-dependent properties, a similar approach to the example given on redox reaction was used. The potential of the system as a function of time, $E_{(t)}$, is written as in (19).

$$E_{(t)} = |v_b t + E_{rev} - E_{init}| + E_{rev} - E^o \tag{19}$$

By setting the scan rate, v_b at a low value of 1×10^{-6} V/s a slow reaction time like steady state situation was simulated. This was translated into the software transient program of the time step, t_{step}, and end time, t_{end}. The equations used for the mentioned parameters are given in (20) and (21).

$$t_{end} = \frac{(E_{init} - E_{rev})}{v_b} \times 2 \tag{20}$$

$$t_{step} = \frac{t_{end}}{no. of\ calculation} \tag{21}$$

The standard potential, E^0 is specific to the types of electrodes and the mechanistic steps. For example $(E^0{}_V)_{TiC}$ indicates the standard potential of the Volmer step for the TiC electrode (shown in Table 2). This simulation is modeled to emulate the experimentation of HER where it is known that the cathodic formation of hydrogen occurs at 0 V (examples given by Zubair et al. [25]). Lasia [21] stated that it is much simpler to refer working potentials to the HER equilibrium which is 0 V.

Table 2. Summary of VHT kinetic parameters obtained in simulation

Materials		B	Mo	Mo$_2$B	α-MoB	β-MoB	MoB$_2$
Boron content		100	0	5.33	10.13		18.4
	k_V	9.0×10^{-4}	6.0×10^{-5}	9.0×10^{-6}	3.0×10^{-6}	1.5×10^{-5}	8.0×10^{-6}
Volmer kinetics parameters	k_{-V}	9.0×10^{-1}	6.0×10^{-2}	9.0×10^{-3}	3.0×10^{-3}	1.5×10^{-2}	8.0×10^{-3}
	β_V	0.24	0.35	0.58	0.79	0.85	0.85
	k_H	1.0×10^{-4}	5.0×10^{-5}	5.0×10^{-5}	4.0×10^{-6}	8.0×10^{-5}	8.0×10^{-5}
Heyrovsky kinetics parameters	k_{-H}	1.0×10^{-1}	5.0×10^{-2}	5.0×10^{-2}	4.0×10^{-3}	8.0×10^{-2}	8.0×10^{-2}
	β_H	0.21	0.33	0.54	0.85	0.29	0.29
Tafel kinetic parameters	k_T	0	0	0	0	1×10^8	1×10^9
	k_{-T}	0	0	0	0	1×10^8	1×10^9
Mechanistic steps		V-H	V-H	V-H	V-H	V-H-T	V-H-T

3. RESULTS AND DISCUSSION

3.1. Kinetic parameters and current density at 10 mA/cm^2

This work has provided kinetic insight into the molybdenum boride surfaces (reaction intermediates, reaction pathways, and rate-determining steps, which are crucial for designing efficient catalysts). The study was able to predict the behavior of molybdenum borides during the HER by determining the electrochemical steps standard rate constant of V, H, and the chemical reaction step rate constant of T (given in Table 2).

The utilization of MoB$_2$ as a catalyst in electrocatalysis has garnered significant attention due to its exceptional properties, specifically in terms of its standard rate constant and charge transfer coefficient. The efficient conversion of reactants is facilitated by the rapid. The current density (mA/cm^2) holds significant importance in determining the efficacy and effectiveness of electrochemical processes, especially electrolyzers. A good-performing electrocatalyst would exhibit a high current density value. Figure 2 show the comparison of experimental and simulation findings of the current density of Mo, B, Mo$_2$B, α-MoB, β-MoB, and MoB$_2$.

The plotted graph proves the coherency between the experimental and simulation findings. The dotted experimental curves show that the experimental data were limited to -3.5 to 5 mA/cm^2. By adopting the VHT model the simulation was able to predict the overpotential at 10 mA/cm^2, η_{10} recorded at approximately 880, 680, 560, 350, 310, and 298 mV for B, Mo, Mo$_2$B, α-MoB, β-MoB, and MoB$_2$ respectively. This result shows that MoB$_2$ was able to achieve convincing current density values for a transition metal catalyst. The obtained standard rate constant data given in Table 3 has proven to be a good numerical estimation and reference for electrocatalyst physical modeling. Our research shows that the Tafel step exists at higher kinetics this was shown by β-MoB and MoB$_2$ exhibiting VHT steps. Future research may look into altering the material surface to produce a catalyst with a high surface area.
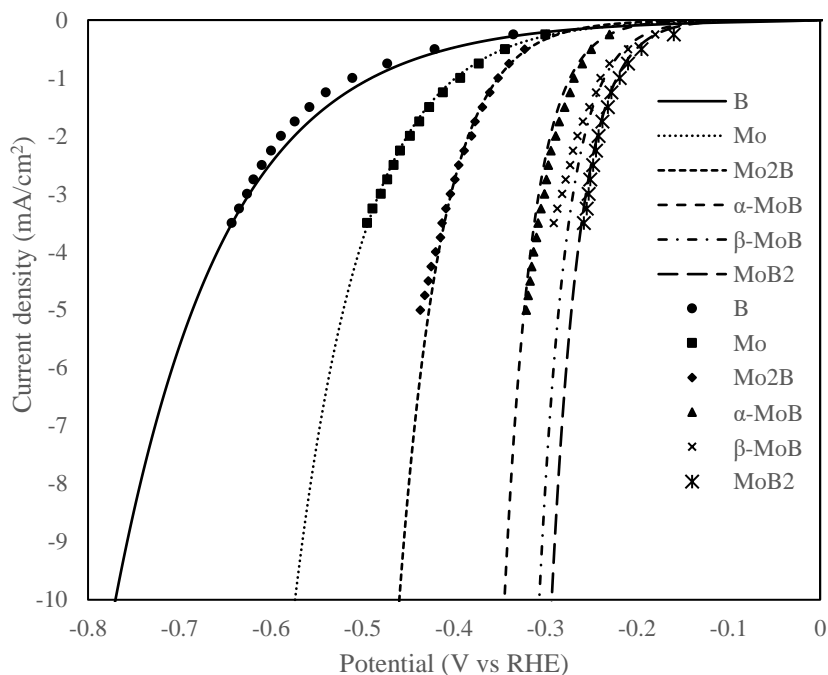
Figure 2. Polarization curves for amorphous B, Mo, Mo$_2$B, α-MoB, β-MoB, and MoB$_2$ in 0.5 M H$_2$SO where solid lines are the experimental curves (Park *et al*. [4]) and dotted plots are the simulation curves

3.2. Tafel plots

The log$_{10}$ of current density, *j* (in mA/cm^2) is generally known as the T plots. It is a graphical representation of the kinetic of electrochemical reactions in multiple electrochemical systems including HER. Figure 3 shows the comparison of experimental plots by Park *et al*. [4] and the simulation plots by this study. The simulation lines were plotted from 0 to -0.5 V while the experimental lines were plotted in the region of -1 to 1 of log10 (j) in mA/cm^2.
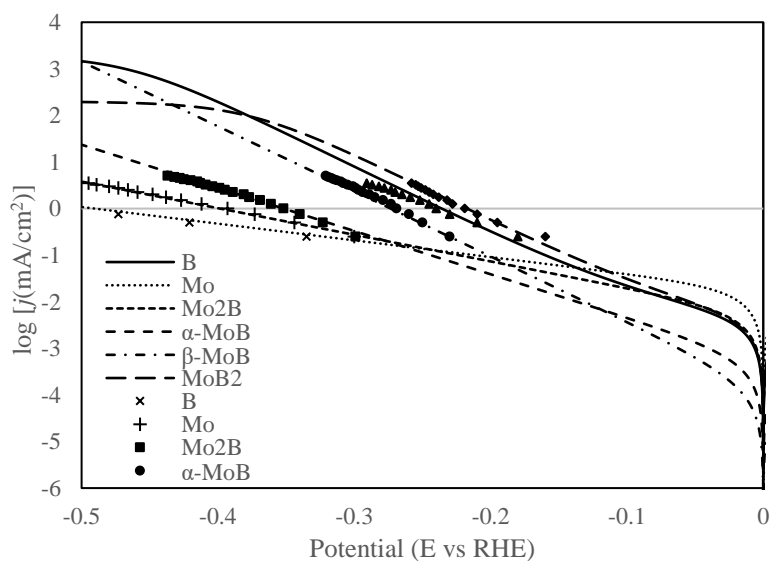
Figure 3. The corresponding T plots of B, Mo, Mo$_2$B, α-MoB, β-MoB, and MoB$_2$ scan rate was 1 mV/s in 0.5 M H$_2$SO$_4$ where solid lines are the experimental curves (Park *et al*. [4]) and dotted plots are the simulation curves

Kinetic study and simulation of molybdenum borides for hydrogen evolution reaction (Harunal Rejan Ramji)

Murthy *et al*. [26] proposed that the T constant can be considered as the onset potential of HER. The T constant becomes the defining parameter between two electrocatalysts when other parameters such as the T slope or exchange current density become the same. The intrinsic reaction rates of the V and H reactions are represented by the standard rate constants kV and kH, respectively. The kinetics of the reactions are determined by these constants, which exhibit a direct correlation with the T plot. An increased value of kV and kH denotes an augmented reaction rate, which leads to more pronounced inclines in the T plot. An electrocatalyst that possesses higher values of kV and kH demonstrates an increased level of catalytic activity, which is evidenced by higher current densities for a given applied potential. The presence of the Tafel step was evident on a plateau-like plot as shown by MoB2 stagnation from -0.35 to -0.5 V. The HER performances of the studied catalyst are summarized in Table 3.

Table 3. Summary of the HER performances of the electrocatalysts

Materials	Tafel slope (mV/dec)		Overpotentials at 3.5 mA/cm^2, $\eta_{3.5}$ (mV) [4]	Overpotentials at 10 mA/cm^2, η_{10} (mV) (simulation-present study)	Exchange current density, j_o (mA/cm^2) (simulation-present study)
	Exp [4]	Sim			
B	-	270	650	780	6.31×10^{-3}
Mo	-	180	500	585	3.16×10^{-3}
Mo$_2$B	128	100	420	480	3.98×10^{-4}
α-MoB	76	80	310	350	
β-MoB	84	70	290	310	
MoB$_2$	75	60	270	300	7.94×10^{-4}

4. CONCLUSION

Recent observations indicate that boron exhibits a T slope of 270 mV/dec, slow reaction kinetics, and high energy requirements for electrochemical processes. Mo follows with a T slope of 180 mV/dec, suggesting slightly better electrochemical kinetics and lower activation energy compared to boron. Mo$_2$B demonstrates a lower T slope of 100 mV/dec, indicating even more favorable kinetics and energetically favorable reactions. Finally, MoB$_2$ exhibits the lowest T slope of 60 mV/dec, indicating highly favorable kinetics and efficient electrochemical processes. Our findings offer definitive proof that the simulated results show that B, Mo, Mo$_2$B, and α-MoB, proceed through V-H mechanistic steps (slower kinetics) while β-MoB and MoB$_2$ exhibit V-H-T mechanistic steps with higher kinetics. The kinetic parameters were determined in terms of the standard rate constant parameters for the Volmer step (k$_V$, k$_{-V}$), Heyrovsky step (k$_H$, k$_{-H}$), and rate constant for the Tafel step (K$_T$, K$_{-T}$). The simulation was able to predict the overpotential at 10 mA/cm^2, η_{10} recorded at approximately 780, 585, 480, 350, 310, and 300 mV for B, Mo, Mo$_2$B, α-MoB, β-MoB, and MoB$_2$ respectively. Boron exhibits slower reaction kinetics and higher energy requirements, making it less efficient as an electrocatalyst compared to Mo, Mo$_2$B, α-MoB, β-MoB, and MoB$_2$. Based on these findings, the adopted mathematical model shows good coherency to the experimental findings. Given the importance of designing an electrocatalyst for HER, this work sheds light on the mathematical approach to understanding the VHT steps. The simulation work provides a good numerical estimation of the characteristics of the electrocatalyst for HER.

REFERENCES

[1]   M. Miao, J. Pan, T. He, Y. Yan, B. Y. Xia, and X. Wang, "Molybdenum carbide-based electrocatalysts for hydrogen evolution reaction," *Chemistry – A European Journal*, vol. 23, no. 46, pp. 10947–10961, Aug. 2017, doi: 10.1002/chem.201701064.
[2]   X. Wang, G. Tai, Z. Wu, T. Hu, and R. Wang, "Ultrathin molybdenum boride films for highly efficient catalysis of the hydrogen evolution reaction," *Journal of Materials Chemistry A*, vol. 5, no. 45, pp. 23471–23475, 2017, doi: 10.1039/C7TA08597D.
[3]   P. R. Jothi, Y. Zhang, J. P. Scheifers, H. Park, and B. P. T. Fokwa, "Molybdenum diboride nanoparticles as a highly efficient electrocatalyst for the hydrogen evolution reaction," *Sustainable Energy & Fuels*, vol. 1, no. 9, pp. 1928–1934, 2017, doi: 10.1039/C7SE00397H.
[4]   H. Park, A. Encinas, J. P. Scheifers, Y. Zhang, and B. P. T. Fokwa, "Boron-dependency of molybdenum boride electrocatalysts for the hydrogen evolution reaction," *Angewandte Chemie International Edition*, vol. 56, no. 20, pp. 5575–5578, May 2017, doi: 10.1002/anie.201611756.
[5]   C. Jian, Q. Cai, W. Hong, J. Li, and W. Liu, "Edge-riched MoSe 2 /MoO 2 hybrid electrocatalyst for efficient hydrogen evolution reaction," *Small*, vol. 14, no. 13, Mar. 2018, doi: 10.1002/smll.201703798.

[6]   J. Zhang *et al.*, "Accelerated hydrogen evolution reaction in CoS 2 by transition-metal doping," *ACS Energy Letters*, vol. 3, no. 4, pp. 779–786, Apr. 2018, doi: 10.1021/acsenergylett.8b00066.

[7]   L. Zhang *et al.*, "One-pot synthesized boron-doped RhFe alloy with enhanced catalytic performance for hydrogen evolution reaction," *Applied Catalysis B: Environmental*, vol. 230, pp. 58–64, Aug. 2018, doi: 10.1016/j.apcatb.2018.02.034.

[8]   F. Safizadeh, E. Ghali, and G. Houlachi, "Electrocatalysis developments for hydrogen evolution reaction in alkaline solutions – A Review," *International Journal of Hydrogen Energy*, vol. 40, no. 1, pp. 256–274, Jan. 2015, doi: 10.1016/j.ijhydene.2014.10.109.

[9]   I. Danaee and S. Noori, "Kinetics of the hydrogen evolution reaction on NiMn graphite modified electrode," *International Journal of Hydrogen Energy*, vol. 36, no. 19, pp. 12102–12111, Sep. 2011, doi: 10.1016/j.ijhydene.2011.06.106.

[10]   O. Azizi, M. Jafarian, F. Gobal, H. Heli, and M. G. Mahjani, "The investigation of the kinetics and mechanism of hydrogen evolution reaction on tin," *International Journal of Hydrogen Energy*, vol. 32, no. 12, pp. 1755–1761, Aug. 2007, doi: 10.1016/j.ijhydene.2006.08.043.

[11]   Y. Luo, Y. Guan, G. Liu, Y. Wang, J. Li, and L. Ricardez-Sandoval, "First-principles-based kinetic monte carlo model of hydrogen evolution reaction under realistic conditions: solvent, hydrogen coverage and electric field effects," *ACS Catalysis*, vol. 14, no. 4, pp. 2696–2708, Feb. 2024, doi: 10.1021/acscatal.3c04588.

[12]   A. Lasia and A. Rami, "Kinetics of hydrogen evolution on nickel electrodes," *Journal of Electroanalytical Chemistry and Interfacial Electrochemistry*, vol. 294, no. 1–2, pp. 123–141, Nov. 1990, doi: 10.1016/0022-0728(90)87140-F.

[13]   P. Los, A. Rami, and A. Lasia, "Hydrogen evolution reaction on Ni-Al electrodes," *Journal of Applied Electrochemistry*, vol. 23, no. 2, Feb. 1993, doi: 10.1007/BF00246950.

[14]   W. Xu *et al.*, "Experimental and computational insight into the role of cobalt and phosphorus in boosting Volmer and Heyrovsky steps of Ni in alkaline hydrogen evolution reaction," *Fuel*, vol. 358, p. 130174, Feb. 2024, doi: 10.1016/j.fuel.2023.130174.

[15]   M. T. Tang, X. Liu, Y. Ji, J. K. Norskov, and K. Chan, "Modeling hydrogen evolution reaction kinetics through explicit water–metal interfaces," *The Journal of Physical Chemistry C*, vol. 124, no. 51, pp. 28083–28092, Dec. 2020, doi: 10.1021/acs.jpcc.0c08310.

[16]   M. López, K. S. Exner, F. Viñes, and F. Illas, "Theoretical study of the mechanism of the hydrogen evolution reaction on the V2C MXene: Thermodynamic and kinetic aspects," *Journal of Catalysis*, vol. 421, pp. 252–263, May 2023, doi: 10.1016/j.jcat.2023.03.027.

[17]   M. D. Makhafola *et al.*, "Palladinized graphene oxide-MOF induced coupling of Volmer and Heyrovsky mechanisms, for the amplification of the electrocatalytic efficiency of hydrogen evolution reaction," *Scientific Reports*, vol. 11, no. 1, p. 17219, Aug. 2021, doi: 10.1038/s41598-021-96536-9.

[18]   J.-P. Diard, B. Le Gorrec, and C. Montella, "Non-linear impedance for a two-step electrode reaction with an intermediate adsorbed species," *Electrochimica Acta*, vol. 42, no. 7, pp. 1053–1072, Jan. 1997, doi: 10.1016/S0013-4686(96)00206-X.

[19]   L. R. Faulkner, H. S. White, and A. J. Bard, *Electrochemical Methods: Fundamentals and Applications, 2nd Edition*, 3rd ed. John Wiley & Sons, 2022.

[20]   E. Kemppainen, J. Halme, O. Hansen, B. Seger, and P. D. Lund, "Two-phase model of hydrogen transport to optimize nanoparticle catalyst loading for hydrogen evolution reaction," *International Journal of Hydrogen Energy*, vol. 41, no. 18, pp. 7568–7581, May 2016, doi: 10.1016/j.ijhydene.2015.12.207.

[21]   A. Lasia, "Mechanism and kinetics of the hydrogen evolution reaction," *International Journal of Hydrogen Energy*, vol. 44, no. 36, pp. 19484–19518, Jul. 2019, doi: 10.1016/j.ijhydene.2019.05.183.

[22]   N. Glandut, A. D. Malec, M. V. Mirkin, and M. Majda, "Electrochemical studies of the lateral diffusion of TEMPO in the aqueous liquid/vapor interfacial region," *The Journal of Physical Chemistry B*, vol. 110, no. 12, pp. 6101–6109, Mar. 2006, doi: 10.1021/jp0570824.

[23]   N. Glandut, C. F. Monson, and M. Majda, "Electrochemistry of TEMPO in the aqueous liquid/vapor interfacial region: measurements of the lateral mobility and kinetics of surface partitioning," *Langmuir*, vol. 22, no. 25, pp. 10697–10704, Dec. 2006, doi: 10.1021/la061172y.

[24]   R. G. Compton and C. E. Banks, *Understanding Voltammetry*, 3rd ed. WORLD SCIENTIFIC (EUROPE), 2018. doi: 10.1142/q0155.

[25]   M. Zubair, M. M. Ul Hassan, M. T. Mehran, M. M. Baig, S. Hussain, and F. Shahzad, "2D MXenes and their heterostructures for HER, OER and overall water splitting: A review," *International Journal of Hydrogen Energy*, vol. 47, no. 5, pp. 2794–2818, Jan. 2022, doi: 10.1016/j.ijhydene.2021.10.248.

[26]   A. P. Murthy, J. Theerthagiri, and J. Madhavan, "Insights on tafel constant in the analysis of hydrogen evolution reaction," *The Journal of Physical Chemistry C*, vol. 122, no. 42, pp. 23943–23949, Oct. 2018, doi: 10.1021/acs.jpcc.8b07763.

BIOGRAPHIES OF AUTHORS

Harunal Rejan Ramji 🆔 ⑧ SC ↻ is a lecturer in the Department of Chemical Engineering and Energy Sustainability, Faculty of Engineering at Universiti Malaysia Sarawak (UNIMAS). He received his Ph.D. in ceramic materials and surface treatments from the University of Limoges (UNILIM), France. His research interests are numerical modeling and electrocatalysis. He can be contacted at email: rhrejan@unimas.my.

Muhammad Qhaliff Zainal Ibidin received his bachelor's degree in Department of Chemical Engineering and Energy Sustainability, Faculty of Engineering, Universiti Malaysia Sarawak (UNIMAS) in 2023. His research interest includes numerical modeling and electrocatalysis. He can be contacted at email: alipzainal99@gmail.com.

Nicolas Glandut is his Ph.D. In electrochemistry from the Grenoble Institute of Technology in 2004. In 2001, he graduated from the same institute with an engineer's degree in electrochemistry. After a postdoctoral stay with Professor Majda at the University of California Berkeley in 2005 and 2006, he returned to France to join the European Ceramics Center in Limoges, as a Maître de conférences (equivalent to Associate Professor). His research now focuses on electrochemistry and laser irradiation of non-oxide ceramics, to develop new systems for energy storage and conversion. He can be contacted at email: nicolas.glandut@unilim.fr.

Joseph Absi is an experienced professor in the Mechanical and Production Engineering Department at the University of Limoges (UNILIM). Skilled in numerical modeling and ceramic materials. He had over 25 years of working experience in teaching and research. His research interest includes numerical calculations of ceramic materials. He can be contacted at email: joseph.absi@unilim.fr.

Lim Soh Fong is a Professional Engineer (PEng) registered with the Board of Engineer Malaysia (BEM), a Chartered Engineer (CEng) of the Engineering Council, UK, and a Chartered Chemical Engineer, Chartered Member (MIChemE) of Institution of Chemical Engineers (IChemE), UK. She is also the founding Chief Editor and Chief Editor of the Journal of Applied Science and Process Engineering. She received her Bachelor's Degree with First Class Honors in Department of Chemical Engineering and Energy Sustainability, Faculty of Engineering, Universiti Teknologi Malaysia in 2003. She obtained her Doctor of Philosophy (Ph.D.) Degree from the National University of Singapore in 2008. Her research interests are in the area of water and wastewater treatment, the interaction of metal and organic compounds in soil and marine environments, the recovery of natural and waste resources, the adsorption process (separation), and green material technology. She can be contacted at email: sflim@unimas.my.